Title: The anatomical pathways for antennal sensory information in the central nervous system of the cricket, *Gryllus bimaculatus*

Author: Atsushi Yoritsune, Hitoshi Aonuma*

Institutional Affiliations: Research Institute for Electronic Science, Hokkaido University, Sapporo, 060-0812, Japan

Abbreviated Title: Antennal information processing pathway in the cricket

Key Words: Insect, brain, antennal lobe, dorsal lobe, projection neuron

*Corresponding Author: Hitoshi Aonuma, DSc.
Address: Research Institute for Electronic Science, Hokkaido University, Sapporo 060-0812, Japan.
Phone: +81-(0)11-706-3832, Fax: +81-(0)11-706-4971
E-mail: aon@es.hokudai.ac.jp

List of Abbreviations

α: α-lobe of the mushroom body, AACT: accessory antenno-cerebral tract, ACT: antenno-cerebral tract, adLH: antero-dorsal lateral horn, AL: antennal lobe, ALPN: projection neuron originating from the antennal lobe, Ant: anterior, avLH: antero-ventral lateral horn, β: β-lobe of the mushroom body, CA: anterior calyx of the mushroom body, CC: central complex, CP: posterior calyx of the mushroom body, DL: dorsal lobe, Dors: dorsal, dPr: dorsal protocerebrum, IACT: inner antenno-cerebral tract, idPr: inferior dorsal protocerebrum, ilPr: inferior lateral protocerebrum, IS: isthmus, Lat: lateral, LH: lateral horn, OACT: outer antenno-cerebral tract, pdLH: postero-dorsal lateral horn, PN: projection neuron, SoG: suboesophageal ganglion, VFA: ventral area of flagellar afferents, VFAPN: projection neuron originating from the ventral area of flagellar afferents, vlPr: ventro-lateral protocerebrum, VT: visual tract, UT: unknown tract

Abstract

Antennae are one of the major organs to detect chemo- and mechano-sensory cue in crickets. Little is known how crickets process and integrate different modality of information in the brain. We thus used a number of different anatomical techniques to gain an understanding of the neural pathways extending from the antennal sensory neurons up to centers in the brain. We identified 7 antennal sensory tracts (assigned as T1-7) utilizing anterograde dye filling from the antennal nerve. Tracts T1-T4 project into the antennal lobe (AL), while tracts T5 and T6 course into the dorsal region of the deutocerebrum or the suboesophageal ganglion, and finally tract T7 terminates in the ventral area of flagellar afferent (VFA). By analyzing autofluorescence images of the AL, we identified 49 sexually isomorphic glomeruli on the basis of shape, relative position and size. On the basis of our sensory-tract data we assigned the glomeruli into one of four separate groups. We then three-dimensionally reconstructed the internal structures in the AL (glomeruli) and the VFA (layers). Next in the protocerebrum we identified both the tracts and their

terminations from the AL and VFA. We found that 10 tracts originate in the AL, whereas there are at least eight tracts from the VFA. Several tracts from the AL share their routes with those from the VFA, but their termination areas are segregated. We now have a better anatomical understanding of the pathways for the antennal information in cricket.

Introduction

Antennal sensory information that contain chemical and tactile sensory information is crucial for insects, for example to find their foods, to find mating partner and to detect threat. However, the neuronal mechanism underlying chemical information processing in crickets, including environmental chemicals, pheromones and other stimuli, remains still unclear. Male crickets, for example, recognize a conspecifics' sexuality using antennal sensory information. Males show aggressive behavior towards approaching males, whereas they exhibit courtship behavior with females (Alexander, 1961; Simmons, 1986; Nagao and Shimozawa, 1987; Adamo and Hoy, 1995). Chemical cues on the body surface are necessary for sexual recognition (Tregenza and Wedell, 1997; Nagamoto et al., 2005), but tactile cues also play an important role (Adamo and Hoy, 1995; Hofmann and Schildberger, 2001). It is thought that males integrate both antennal chemical and tactile cues in their CNS to 'decide' whether to act either in an aggressive or courtship manner. However, our understanding how they process and integrate these cues in the brain is

lacking, due in part to uncertainty of the anatomical pathways involved in the decision making process. Thus, we set out to elucidate both the pathways and central anatomical structures involved in this decision making process.

Chemical sensory afferents terminate in the antennal lobe (AL); whereas, most of exteroceptive mechanosensory afferents terminate in the dorsal lobe (DL) of the brain (Homberg et al., 1989). The AL consists of multiple islets of neurons, known as glomeruli, which can be thought of as the functional units of olfaction. There are great similarities across species regarding the arrangement of the glomeruli (moth: Rospars and Hildebrand, 1992; honeybee: Flanagan and Mercer, 1989; fly; Laissure et al., 1999; cockroach: Chiang et al., 2001). However, there are sexual dimorphic differences in the AL within species and this dimorphism may underlie the differences in processing sex pheromone odors (Burrows et al., 1982; Christensen and Hildebrand, 1987; Kondoh et al., 2003). The terminals of olfactory sensory afferents that express the same odorant receptor or that have a similar response profile converge in the same glomeruli (Gao et al., 2000; Vosshall et al., 2000; de

Bruyne et al., 2001).

In a number of different species, the chemical information having been processed by local interneurons in the AL, is sent up to 'higher centers' (the calyx of the mushroom body, and the lateral protocerebrum) by projection neurons (PNs) via several neuronal tracts, known as the antenno-cerebral tracts (ACTs) (moth: Homberg et al., 1988; Rø et al., 2007; cockroach: Malun et al., 1993; honeybee: Kirchner et al., 2006; ant: Zube et al., 2008). In *G. bimaculatus*, however, only a part of projection routes and terminating regions of the PNs are known (Frambach et al., 2004; Frambach and Schürmann, 2004). We therefore need a far more detailed description of the anatomical pathways subserving antennal sensory information processing.

The anatomical pathways involved in mechanical information in a wide variety of insects are known. The DL receives exteroceptive and proprioceptive mechanical information from the antenna, and may relay it to antennal motor neurons (fly: Burkhardt and Gewecke, 1965; honeybee: Kloppenburg, 1995) and descending neurons (cockroach:

Burdohan and Comer, 1996). However, the situation in the cricket is not so clear. There is an area in the deutocerebrum known as “the ventral area of the flagellar afferents (VFA)” that is a multi-layered neuropil, where antennae flagellar mechanosensory neurons terminate (Staudacher and Schildberger, 1999; Staudacher et al., 2005). Multiple layers of the VFA are thought to serve as a somatotopic representation of the antenna (Staudacher and Schildberger, 1999; Gebhardt and Honegger, 2001). Moreover, the pathways from the DL and/or the VFA into the protocerebrum have also not been well investigated (cricket: Staudacher et al., 2005; cockroach: Malun et al., 1993). However, it is clear that exteroceptive and proprioceptive mechanical information must be sent to protocerebrum, because neurons there respond to antennal mechanical stimulation (cricket: Schildberger, 1984; cockroach: Mizunami et al., 1998; Okada et al., 1999).

We undertook this present study to demonstrate the anatomical pathways used by crickets to process antennal chemical and mechanical information.

Materials and Methods

Animals

Crickets *Gryllus bimaculatus* (DeGeer) were reared in plastic cases (80cm × 45 cm × 20 cm) on a 14h : 10h light and dark cycle at 28 ± 2ºC. They were fed a diet of insect food pellet (Oriental Yeast Co., Tokyo, Japan), chopped carrot and water *ad libitum*. Adult crickets that had molted for 2-4 weeks before the experiment were used in this study.

Anatomical experiments

We used three different preparations in this report: 1) anterograde dye filling of the antennal nerve, 2) autofluorescence intensification, 3) extracellular tracer application into the AL or the VFA.

Anterograde dye filling of the antennal nerve. Crickets were tethered with small slips of Parafilm (American National Can, IL, USA) and had plastic tubes implanted into their neck. Antennae were cut at the lower part of flagellum, and the cut ends were

washed with cricket saline containing EDTA to prevent the blood from clotting. Plastic pipettes containing 5 μl of 5% neurobiotin in 0.1 M phosphate buffer saline (PBS) (pH 7.4) in the tips were slipped over the antennae. Then the animals were stored in a moist chamber at 4 ºC for 2 days. After the agent was anterogradely transported, the brains were dissected out from the head capsule in a cooled cricket physiological saline (140 mM NaCl, 10 mM KCl, 1.6 mM $CaCl_2$, 2 mM $MgCl_2$, 44 mM Glucose, 2 mM TES, pH 7.2). They were fixed with 4% paraformaldehyde in PBS overnight at 4ºC. After washing with 0.2% Triton X-100 in PBS (PBS-TX) for 3 hrs, they were incubated in PBS-TX containing streptavidin-Cy3-conjugate or streptavidin-Cy2-conjugate (1:200) overnight at 4 ºC. After wash with PBS-TX (for 15 min, by 4 times) and PBS (for 30 min, by 4 times), they were dehydrated with ethanol series (70, 80, 90, 95, 100%; for 10 min respectively), and cleared with methyl salicylate.

Autofluorescence intensification. For visualization of brain structures, we utilized tissue autofluorescence caused by glutaraldehyde fixatio. Brains were dissected out

in cricket saline, fixed in 0.1% glutaraldehyde for 3-5 days at 4 ºC, dehydrated with ethanol series, and cleared with methyl salicylate.

Extracellular tracer application. For identification of the projection tracts and areas of the neurons, fluorescent tracer was applied in the deutocerebrum. Brains of male crickets were isolated in the cricket saline, and fixed on a Sylgard-lined Petri dish with insect pins. The brain sheath of the deutocerebrum was partly ripped open with sharpened forceps. A glass micropipette (outer diameter 1.2 mm, inner diameter 0.75 mm; Narishige, Tokyo, Japan) pulled with a laser puller (P-2000, Sutter Instrument, Novato, CA) was filled with 3% Lucifer yellow-CH (Sigma-Aldrich, St. Louis, MO) diluted in 0.1 M LiCl. The micropipette, the tip of which was slightly broken, was inserted into the deutocerebrum. The dye was iontophoretically injected by 10 nA hyperpolarizing current for 10-30 min. Before withdrawing, the dye was allowed to diffuse into neurons for several minutes. Then preparations were fixed with 4% paraformaldehyde in PBS for 1-2 hr, dehydrated in ethanol series, and cleared with methyl salicylate.

Data analysis

Cleared brains were mounted as whole-mounts on custom-made cover slips filled with methyl salicylate. Images were observed and captured with a confocal laser-scanning microscope (CLSM; FV-1000, Olympus, Tokyo, Japan) as consecutive optical sections with a 0.5-2 μm interval, using an UPlanSApo (×10/0.40, ×20/0.75) objective lens. Identification of the antennal sensory tracts, glomeruli, and layers were done using consecutive optical sections of the entire deutocerebrum. All morphological descriptions referred to the embryonic neuroaxis, which is tilted by approximately 90º with respect to the head-body axis. Sensory tracts were identified by comparing the position and branching pattern reported in previous reports in the honeybee (T1-T6; Suzuki, 1975) and cricket (T7; Staudacher and Schildberger, 1999). Therefore we followed the nomenclature of antennal tracts in naming sensory tracts. Glomeruli in the AL were identified on the basis of shape, relative size and location. By comparing stacked images of autofluorescence and dye filling from antennal nerve, we grouped and named the glomeruli

to the corresponding to the tracts that terminated in each. Thus, we designated glomeruli A as the structure to which axons in T1 terminated in, and, likewise, B for T2, C for T3, D for T4, etc.. The classification of antenno-cerebral tracts (ACTs) was mostly based on published data from cockroach (Malun et al., 1993). We defined the lateral horn (LH) as a neuropil that receives the majority of terminals of the PNs from the AL through inner the antenno-cerebral tract (ACT).

Results

Identification of sensory tracts

Dye-filling experiments on the antennal nerve (N = 15: 10 males and 5 females) showed that there are 7 major antennal sensory tracts named T1-T7 respectively (Fig 1). Four tracts (T1-T4) were found to project into the antennal lobe (AL) (Suppl 1). The terminals of the sensory afferents form glomerulus at the AL (Fig 2). Each glomerulus was

observed to contain internal fine glomerular substructures, which we have called "micro-glomerular structure" (Fig 2A). T1 ran along ventral boundary of the AL and terminated in glomeruli covering the ventral area (Fig 1B, 2B). T2 ran more dorsal to T1, along the anterior boundary of the AL and terminated primarily in glomeruli located in the lateroposterior area (Fig 1C). T3 ran along the posterior boundary of the AL and terminated predominately in glomeruli located in the postero-ventral area (Fig 1C). T4 ran along the dorsal boundary of the AL and terminated in glomeruli covering the most dorsal area (Fig 1D). T4 nerve bundle descended to the medial part of the VFA (arrow in Fig 1D), and a portion of them terminated in the suboesophageal ganglion (SoG) together with those of T6 (Fig 1F). In addition a second T4 nerve bundle ran along the dorsal boundary of the AL with some collaterals (IS in Fig 1D, 2 B) and turned antero-ventrally thus terminating in the medio-ventral region of the protocerebrum (IS in Fig 1B, 2B). T5 and T6 ran together dorsal to the AL. T5 nerve bundles terminated in the DL, while those in T6 divided into T6-1 and T6-2 in the DL. T6-1 then descended to the SoG (Fig 1E, F), while

sending some collaterals into the dorsal region of the VFA (Fig 1E). T6-2 ran dorso-medially and terminated in the dorso-medial part of the DL (Fig 1E). T7 ran postero-medially and entered into the VFA, the ventral area from the DL (Fig 1C). The projections of antennal sensory neurons are summarized in Fig 2C.

Classification of the glomeruli

CSLM images of autofluorescence of brains revealed that there were 49 glomeruli on each side of the AL (N=19: 12 males and 7 females). Each glomerulus was anatomically identifiable by its shape, relative size, and position (Fig 3). The 49 identified glomeruli were classified into 4 groups on the basis of antennal sensory tracts (T1-T4). There are 8 glomeruli in group A, 16 in group B, 17 in C, and 8 in D. The glomeruli located in the ventral part of the AL (i.e. A, B, and C) are more compactly arranged than those in the dorsal part (D). More dorsal to the glomeruli in the D group, 3 additional neuropils were found where antennal sensory afferents projecting through T4 terminate. We did not

classify them as glomeruli, but classified them as “isthmi” (IS in Fig 1D, 2B). We compared selected CSLM stacks of right and left ALs from 12 males and 7 females. There was little variation in the arrangement of the glomeruli (male: Fig 4A, B; female Fig 4C, D). However, some degree of inter-individual variation was observed. For example, the A4, B8, or C1 glomerulus was sometimes observed to be subdivided (3 in 12 males, 2 in 7 females), and B3 and B5 were sometimes observed to be fused (2 in 12males, 1 in 7 females).

The layers in the ventral area of flagellar afferents (VFA)

Dye-filled afferent antennal fibers were arranged in parallel layers in the VFA (Fig 5). T7 fibers ran medio-posteriorly in the postero-ventral surface of the deutocerebrum and then terminate in the VFA forming five layers in the crickets (N=10: 5 males and 5 females) (Fig 5A, B). The horizontal width of each layer was ~ 90 μm, the vertical width ranged between 25-45 μm, and the medio-posterior thickness ranged between 5-30 μm. We

observed 5 separate fluorescence intensive peaks and these reflect the density of terminals (Fig 5C). The intensity of the florescent signal tended to be weaker in the more lateral layers (Fig 5C). Additionally, the layers appeared to be arranged in sub-compartments, especially in the most medial layer. Their two layered sub-compartments were closely attached together (encompassed regions in Fig 5A). Finally, we have summarized the projection patterns of the antennal tracts and their termination in the deutocerebrum in Figure 6.

Projecting tracts of the AL-PNs and the VFA-PNs

Using the extracellular tracer application method the projecting tracts of axons originating from the AL were visualized in 20 preparations. We found that the AL-PNs coursed through four tracts, IACT, ACT3, ACT4, and OACT. These PNs predominately terminated in the anterior calyx of mushroom body (CA) and terminated in the lateral protocerebrum (termed the lateral horn; LH in Fig 7). The IACT projected medially from the AL into the

protocerebrum and then bent anteriorly along the midline of the brain. This tract then turned laterally into the medio-posterior protocerebrum, coursed dorsally to the peduncle, slightly posterior to the CA, and then turned posteriorly into the LH (Fig 7A-C). The ACT3 projected out of the AL together with the IACT, but separated from the IACT in the centro-medial protocerebrum and then bent laterally to the ipsilateral LH (Fig 7B). The ACT4 ran out of the AL dorso-anteriorly, then ran anteriorly, and finally bended laterally into the LH (Fig 7B). The OACT initially ran with the ACT4 as they exited the AL, but then diverged antero-laterally from the ACT4 into the LH (Fig 7B). The majority of the AL-PN terminals converged in the CA and the LH.

We found 6 additional AL-PN routes that were previously not reported; these ACTs were defined as accessory ACTs (AACTs) (AACT1-6 in Fig 7A-C). Some VFA-PNs partly projected to the AL and formed part of the AACTs. Tracts AACT1, 2, 4 and 5 separate from the IACT laterally at approximately the same point that the ACT3 separated (Fig 7B, C). From that point, the AACT1 ran antero-laterally and joined the

IACT again in the anterior calyx (Fig 7A). AACT2 also ran antero-laterally and joined IACT in the antero-ventral LH (Fig 7C). AACT4 coursed laterally and project into the sdPr, while sending collaterals into the medial protocerebrum (Fig 7C). AACT5 ran postero-laterally, and then turned antero-laterally to join the IACT (Fig 7C). AACT3 had a characteristic trajectory lateral to the IACT and turned laterally to join the ACT3 (Fig 7B). AACT6 emanated from the AL together with the OACT, but then separated more dorso-anteriorly and terminated in the sdPr (Fig 7C).

We next focused our attention on the VFA in 18 preparations. This enabled us to visualize the projecting tracts of axons originating from the AL. We found the VFA-PNs have processes in 3 tracts, ACT3, ACT4, and OACT. These processes predominately terminated in the postero-ventral region of the LH (termed as inferior and superior lateral protocerebrum; ilPr and slPr, respectively in Fig 8A-C). The trajectories of the ACT3, 4, and OACT from the VFA were consistent with those from the AL, but their termination areas were different.

Some of the VFA-PNs were discovered to project through previously unknown routes (AACT3, 4, 6-8). The trajectories of the AACT3, 4, 6 were consistent with those of the AL-PNs. Thus, two new tracts were identified. AACT7 together with IACT sends collaterals into the CA (Fig 8B). AACT8 also emerges from the AL with the IACT, it then turns ventrally, along the ventral surface of the protocerebrum, and finally turns dorso-laterally into the ilPr (Fig 8A). We observed some collateral from the OACT and AACT3 that terminated in the CA (see Fig 8D, E).

Termination areas of the AL-PNs and the VFA-PNs

The extracellular tracer application showed that the AL-PN and the VFA-PN axons terminated in the lateral regions of protocerebrum having sent collaterals into the CA (Fig 7, 8). The axons of the AL-PNs and the VFA-PNs projected similarly their termination areas in the protocerebrum. Ventrally the AL-PNs terminated in the more lateral posterior regions (the LH) than did the VFA-PNs (the slPr and ilPr). Dorsally,

however, the AL-PNs ended in the more posterior region (inferior dorsal protocerebrum; idPr) than did the VFA-PNs (superior dorsal protocerebrum; sdPr).

In the CA, only AL-PN terminals projecting through the IACT were consistently observed, whereas in only some cases were VFA-PN terminals running through the OACT observed. The AL-PN terminations via the IACT were found to arise in the lip region (n = 20), while those VFA-PN terminations via OACT arose from the basal, postero-midial region (Fig 8E). The results of the extracellular tracer application in the AL or VFA are summarized in Fig 9.

Discussion

Terminal of antennal sensory afferents

Retrograde axon tracing of all axons in the antennal nerve of the cricket revealed that antennal sensory afferents are divided into 7 tracts and terminate at the deutocerebrum. We

found previously unknown characteristics of the projection pattern by the antennal tracts to the AL. Four antennal tracts T1-T4 that convey chemical information from the antennae end in the AL. The axon of chemosensory afferents terminate in distinct morphological units named glomeruli where they make synaptic connection with local interneurons, which interconnect subsets of glomeruli, and with PNs that project to the higher information processing centers in the brain. The total number of the glomeruli was 49 in the cricket AL, compared to 50 in the fly (Laissue et al., 1999; Kondoh et al., 2003), 60 in the moth (e.g. Rospars and Hildebrand, 1992; Berg et al., 2002; Sadek et al., 2002) and 92-104 in Hymenopteran species (Smid et al., 2003). The majority of cricket glomeruli contained inner small spheral substructures called 'microglomerular structure' (Ignell et al., 2001). Anatomical analysis in this study demonstrates no sexual dimorphism in the spatial arrangement of the cricket AL, which confirms the previous study by Ignell et al., (2001). A sexual dimorphism in olfactory pathway has been demonstrated in some insects. For example, male insects have sex specific glomeruli, the macroglomerular complex, which

exclusively process information regarding sex pheromones released by conspecific females (cockroach: Burrows et al., 1982; moth: Christensen and Hildebrand, 1987; Kanzaki et al., 1989; fly: Kondoh, 2003; Stockinger et al., 2005). Further, in the moth, female specific glomeruli process odor information concerning host plants (Masante-Roca et al., 2005; Skiri et al., 2005). On the other hand, like crickets some insects have no macroglomerulus (e.g. parasitoid wasps *Cotesiaglomerata and C.rubecula*: Smid et al., 2003). It is demonstrated that ordinary glomeruli in moth also play important role in pheromone information processing (Varela et al., 2011). It is demonstrated that cuticular substances on the body surface of conspecific animals is used for sexual recognition in cricket (Rence and Loher, 1977; Nagamoto et al., 2005). Antennal sensory afferents convey the tactile chomosensory information into the deutocerebrum in cricket. However it is still unclear how and where this information is processed. In *Drosophila*, the spatial arrangement of the glomeruli is sexually isomorphic (Laissue et al., 1999). However, dimorphic functional differences were found using genetic techniques (Stockinger et al., 2005).

We classified the AL glomeruli into four groups (A-D) on the basis of the four sensory tracts (T1-T4). In honeybee, AL is divided into two groups (antero-ventral and postero-dorsal group) on the basis of sensory tract input (T1 and T3). This division is suggested to respond to functional or odotypic grouping in honeybee (Müller et al., 2002; Kirchner et al., 2006). In the most dorsal part of the AL, where T4 terminate, the glomeruli are separated from others, as previously reported (Ignell et al., 2001). This characteristic of T4 is similar to that observed in honeybee (Suzuki, 1975; Galizia et al., 1999).

We found 2 subtracts of T4 in the cricket brain, and could gain new insight to the findings of previous report by Staudacher and Schildberger (1999). One of them projected into the medio-ventral region of the protocerebrum shown as ISs. The IS in the dorsal AL could be analogous to the ‘isthmus’ or ‘knot-like structure’ in moth, which are thought to process mechano-sensory information (Homberg et al., 1988). The other subtracts that projected into the medial area of the VFA are involved with processing exteroceptive mechanosensory information. The VFA was originally defined as a ventral region where

exteroceptive mechanosensory afferents from the antennae flagellum terminated (Staudacher and Schildberger, 1999). The more dorsal region of the VFA receives proprioceptive mechanical sensory information from the pedicel and scape (Gebhardt and Honegger, 2001). The remaining three tracts (T5-T7) therefore convey mechanosensory information as discussed by Staudacher et al. (2005). In the honeybee, T5 contains proprioceptive mechanosensory afferents arising from the scape, whereas T6-1-3 contains afferents arising from Johnstone's organ on the pedicel (Ai et al., 2007). Further more, the DL receives input from both mechano-sensory and gustatory neurons located on the tip of the flagellum in honeybee (Haupt, 2007). In the cockroach, mechanosensory and gustatory afferents on the flagellum terminate in the dorsal part of the DL and the SoG forming three distinct bundles of T6-1, whereas the afferents on the scape and pedicel terminate in the ventral part of the DL (Nishino et al., 2005). T7 is made up of flagellar mechano-sensory afferents in crickets (Staudacher and Schildberger, 1999), whose function is still unclear. The function of the multi-layered neuropil and the arrangements of

sub-compartments in the VFA of the cricket are still remained unclear.

Tracts and termination areas of the AL-PNs

We found that the AL-PNs ran through ten tracts and terminate in the CA and/or the lateral protocerebrum (i.e. LH). Previously the projection patterns of AL-PNs have been investigated in a wide variety of insects (fly: Stocker et al., 1990; cockroach: Malun et al., 1993; moth: Homberg et al, 1988, Rø et al., 2007; honeybee: Kirschner et al., 2006; ant: Zube et al., 2008). As in the other species studied we found in the cricket that the IACT was more frequently and more intensely stained. That is, its axon ran ventral to the peduncle, it sent collaterals into the calyx, and it terminated in the lateral protocerebrum. Almost all of the AL-PNs that project through IACT show uniglomerular arborization in the AL (Schildberger, 1984; Ignell et al., 2001) as they do in other insects (cockroach: Malun et al, 1993; Strausfeld and Li, 1999; honeybee: Abel et al., 2001; Müller et al., 2002; moth: Homberg et al., 1989; Kanzaki et al., 1989; fly: Stocker et al., 1990; Marin et

al., 2002; mosquito: Ignell et al., 2005). In the cockroach, AL-PNs project via ACT2 and there they also exhibit uniglomerular arborization (Malun et al., 1993). However, in the honeybee and moth the AL-PNs project via l-ACT (synonymous with OACT) but also exhibit uniglomerular arborization (Abel et al., 2001; Müller et al., 2002; Rø et al., 2007).

Our finding that the AL-PNs terminate in the CA and/or the LH, confirm previous findings (Frambach and Schürmann, 2004; Frambach et al., 2004) and suggest that these regions are the secondary centers of chemical processing. We found that the AL-PNs projecting through IACT terminated in the CA, whereas the AL-PNs projecting through other ACT or AACT do not terminate in CA. The AL-PNs projecting through IACT directly input onto Kenyon cells in the CA (Frambach et al., 2004).

We found here that almost all of the AL-PNs terminate in the lateral protocerebrum in an area more anteriorly extended than those of other species (e.g. cockroach: Strausfeld and Li., 1999). This difference in where the AL-PNs terminate in the LH of cricket would relate to single calyx morphology. In the cricket, prior to hatching one

of the two clusters of Kenyon cell neuroblast degenerate, leaving only a single calyx in the hemisphere (Cayre et al., 2000; Farris, 2005). Lateral calyx occupies the anterior region of the LH in cricket whereas in cockroach or honeybee this region is where AL-PNs in the IACT terminate.

Tracts and termination areas of the VFA-PNs

For the first time we described that VFA-PNs project to and terminate in the CA and/or the lateral protocerebrum (slPr and ilPr) via 8 tracts. The majority of them project via the OACT. In cockroach, one of the PNs was anatomically described, whose dendrites extended to several dorsal glomeruli of the AL and the DL, and whose axon ran through OACT and terminated in the posterior region of the LH (Malun et al., 1993). This suggested that OACT is a tract transmitting mechanosensory information. Almost all of the VFA-PNs terminate in the slPr or ilPr. Thus, these regions must be secondary mechanosensory centers. In contrast, minorities of the VFA-PNs terminate in the CA,

where mechanosensory information can be combined with olfactory or visual information. Using extracellular tracer application technique we detected terminals in the basal region of the CA from VFA-PNs projecting via OACT. This region can be one of somatosensory center of the insect brain.

Segregation of terminals of the AL-PNs and the VFA-PNs

Both AL-PNs and VFA-PNs project via common routes (i.e. ACT3, ACT4, OACT, AACT3, AACT4, AACT6), however, in other cases AL-PNs project exclusively via (IACT, AACT2, AACT5) and VFA-PNs exclusively via (AACT7, AACT8). In spite of sharing several ACTs, AL-PNs and VFA-PNs terminate in a segregated fashion. Terminals of input neurons are differently distributed in the calyx across sensory modalities. For example, in *G. bimaculatus*, the terminals of AL-PNs and projections from another area (the lobus glomeratus, a putative primary center of palpal gustatory sensory information) are segregated onto the anterior calyx and posterior calyx, respectively (Frambach and

Schürmann, 2004). In like manner in the cockroach, terminals in the calyx of visual and olfactory input neurons are differently distributed (Nishikawa et al., 1998; Strausfeld and Li, 1999). Continuing in this mode odor and mechanical information is combined by Kenyon cells (intrinsic neurons of mushroom body) and multimodal protocerebral neurons (Schildberger, 1984; Li and Strausfeld, 1997; Strausfeld and Li, 1999).

In conclusion, we suggest, both in the primary centers of the deutocerebrum and in higher centers of the protocerebrum, chemical and mechanical information should be represented in spatially segregated neuropils, and this architecture must play an important role in antennal sensory information processing and integration.

ACKNOWLEDGEMENTS

We are grateful to Dr. Lukowiak K. for his critical reading of this manuscript. We also thank Drs. Sakura M. Watanabe T. Hiraguchi T.and Okada R. for their technical supports and for useful discussion. This research was supported by grants-in-aid for Scientific Research (KAKENHI) from the MEXT, Scientific Research on Priority Areas (Area No. 454) to H. Aonuma (No. 17075001) and from the JSPS to H. Aonuma (No. 23300113).

References

Abel R, Rybak J, Menzel R (2001) Structure and response patterns of olfactory interneurons in the honeybee, *Apis mellifera*. J Comp Neurol 437: 363-383

Adamo SA, Hoy RR (1995) Agonistic behaviour in male and female field crickets, *Gryllus bimaculatus*, and how behavioural context influences its expression. Anim Behav 47: 857-868

Ai H, Nishino H, Itoh T (2007) Topographic organization of sensory afferents of Johnston's organ in the honeybee brain. J Comp Neurol 502: 1030-1046.

Alexander RD (1961) Aggressiveness, territoriality, and sexual behaviour in field crickets (Orthoptera: Gryllidae). Behav 17: 130-233

Berg BG, Galizia CG, Brandt R, Mustaparta H (2002) Digital atlases of the antennal lobe in two species of tobacco budworm moths, the oriental *Helicoverpa assulta* (Male) and the American *Heliothis virescens* (Male and Female). J Comp Neurol 446: 123-134

Burdohan JA, Comer CM (1996) Cellular organization of an antennal mechanosensory

pathway in the cockroach, *Periplaneta americana*. J Neurosci 16: 5830-5843

Burkhardt D, Gewecke M (1965) Mechanoreception in arthropoda: the chain from stimulus to behavioral pattern. Cold Spring Harbor Symp quant Biol. 30: 601-614

Burrows M, Boeckh J, Esslen J (1982) Physiological and morphological properties of interneurons in the deutocerebrum of male cockroaches which respond to female pheromone. J Comp Physiol 145: 447-457

Cayre M, Malaterre J, Charpin P, Strambi C, Strambi A (2000) Fate of neuroblast progeny during postembryonic development of mushroom bodies in the house cricket, *Acheta domesticus*. J Insect Physiol 46: 313-319

Chiang A-S, Liu Y-C, Chiu S-L, Hu S-H, Huang C-Y, Hsieh C-H (2001) Three-dimensional mapping of brain neuropils in the cockroach, *Diploptera punctata*. J Comp Neurol 440: 1-11

Christensen TA, Hildebrand JG (1987) Male-specific, sex pheromone-selective projection neurons in the antennal lobe of the moth *Manduca sexta*. J Comp Physiol A 160: 553-569

de Bryune M, Foster K, Carlson JR (2001) Odor coding in the *Drosophila* antenna. Neuron 30: 537-552

Farris SM (2005) Evolution of insect mushroom bodies: old clues, new insights. Arth Struc Dev 34: 211-234

Flanagan D, Mercer AR (1989) An atlas and 3-D reconstruction of the antennal lobes in the worker honey bee, *Apis mellifera* L. (Hymenoptera: Apidae). Int J Insect Morphol Embryol 18: 145-159

Frambach I, Rössler W, Winkler M, Schürmann F-W (2004) F-actin at identified synapses in the mushroom body neuropil of the insect brain. J Comp Neurol 475: 303-314

Frambach I, Schürmann F-W (2004) Separate distribution of deutocerebral projection neurons in the mushroom bodies of the cricket brain. Acta Biol Hung 55: 21-29

Galizia CG, McIlwrath SL, Menzel R (1999) A digital three dimensional atlas of the honeybee antennal lobe based on optical sections acquired by confocal microscopy. Cell Tiss Res 295: 383-394

Gao Q, Yuan B, Chess A (2000) Convergent projections of *Drosophila* olfactory neurons to specific glomeruli in the antennal lobe. Nat Neurosci 3 780-785

Gebhardt M, Honegger H-W (2001) Physiological characterization of antennal mechanosensory descending interneurons in an insect (*Gryllus bimaculatus, Gryllus campestris*) brain. J Exp Biol 204: 2265-2275

Haupt SS (2007) Central gustatory projections and side-specificity of operant antennal muscle conditioning in the honeybee. J Comp Physiol A 193: 523-535

Hofmann HA, Schildberger K (2001) Assessment of strength and willingness to fight during aggressive encounters in crickets. Anim Behav 62: 337-348

Homberg U, Christensen TA, Hildebrand JG (1989) Structure and function of the deutocerebrum in insects. Ann Rev Entomol. 34: 477-501

Homberg U, Montague RA, Hildebrand JG (1988) Anatomy of antenno-cerebral pathways in the brain of the sphinx moth *Manduca sexta*. Cell Tiss Res 254: 255-281

Ignell R, Anton S, Hansson BS (2001) The antennal lobe of Orthoptera: anatomy and

evolution. Brain Behav Evol 57: 1-17

Ignell R, Dekker T, Ghaninia M, Hansson BS (2005) Neuronal architecture of the mosquito deutocerebrum. J Comp Neurol 493: 207-240

Kanzaki R, Arbas EA, Strausfeld NJ Hildebrand JG, (1989) Physiology and morphology of projection neurons in the antennal lobe of the male moth *manduca sexta*. J Comp Physiol A 165: 427-453

Kirschner S, Kleineidam CJ, Zube C, Rybak J, Grünewald B, Rössler W (2006) Dual olfactory pathway in the honeybee, *Apis mellifera*. J Comp Neurol 499: 933-952

Kloppenburg P (1995) Anatomy of the antennal motoneurons in the brain of the honeybee (*Apis mellifera*). J Comp Neurol 363: 333-343

Kondoh Y, Kaneshiro KY, Kimura K, Yamamoto D (2003) Evolution of sexual dimorphism in the olfactory brain of Hawaiian Drosophila. Proc R Soc Lond B 270: 1005-1013

Laissue PP, Reiter C, Hiesinger PR, Halter S, Fischach KF, Stocker RF (1999) Three-dimensional reconstruction of the antennal lobe in *Drosophila melanogaster*. J

Comp Neurol 405: 543-552

Li Y, Strausfeld NJ (1997) Morphology and sensory modality of mushroom body extrinsic neurons in the brain of the cockroach, *Periplaneta americana*. J Comp Neurol 387: 631-650

Malun D, Waldow U, Kraus D, Boeckh J (1993) Connections between the deutocerebrum and the protocerebrum, and neuroanatomy of several classes of deutocerebral projection neurons in the brain of male *Periplaneta americana*. J Comp Neurol 329:143-162

Marin EC, Jefferis GSXE, Komiyama T, Zhu H, Luo L (2002) Representation of the glomerular olfactory map in the *Drosophila* brain. Cell 109: 243-255

Masante-Roca I, Gadenne C, Anton S (2005) Three-dimensional antennal lobe atlas of male and female moths, *Lobesia botrana* (Lepidoptera: Tortricidae) and glomerular representation of plant volatiles in females. J Exp Biol 208: 1147-1159

Mizunami M, Okada R, Li Y, Strausfeld NJ (1998) Mushroom bodies of the cockroach: activity and identities of neurons recorded in freely moving animals. J Comp Neurol 402:

501-519

Müller D, Abel R, Brandt R, Zöckler M, Menzel R (2002) Differential parallel processing of olfactory information in the honeybee, *Apis mellifera* L. J Comp Physiol A 188: 359-370

Nagamoto J, Aonuma H, Hisada M (2005) Discrimination of conspecific individuals via cuticular pheromones by males of the cricket *Gryllus bimaculatus*. Zool Sci 22: 1079-1088

Nagao T, Shimozawa T (1987) A fixed time-interval between two behavioral elements in the mating behaviour of male cricket, *Gryllus bimaculatus*. Anim Behav 35: 122-130

Nishikawa M, Nishino H, Mizunami M, Yokohari F (1998) Function-specific distribution patterns of axon terminals of input neurons in the calyces of the mushroom body of the cockroach, *Periplaneta americana*. Neurosci Lett 245: 33-36

Nishino H, Nishikawa M, Yokohari F, Mizunami M (2005) Dual, multilayered somatosensory maps formed by antennal tactile and contact chemosensory afferents in an

insect brain. J Comp Neurol 493: 291-308

Okada R, Ikeda J, Mizunami M (1999) Sensory responses and movement-related activities in extrinsic neurons of the cockroach mushroom bodies. J Comp Physiol A 185: 115-129

Rence B and Loher W (1977) Contact chemoreceptive sex recognition in the male cricket, *Terelgryllus commodus*. Physiol Entomol 2: 225-236

Rospars JP, Hildebrand JG (1992) Anatomical identification of glomeruli in the antennal lobes of the male sphinx moth *Manduca sexta*. Cell Tiss Res 270: 205-227

Rø H, Müller D, Mustaparta H (2007) Anatomical organization of antennal lobe projection neurons in the moth *Heliothis virescens*. J Comp Neurol 500: 658-675

Sadek MM, Hansson BS, Rospars JP, Anton S (2002) Glomerular representation of plant volatiles and sex pheromone components in the antennal lobe of the female *Spodoptera littoralis*. J Exp Biol 205: 1363-1376

Schildberger K (1984) Multimodal interneurons in the cricket brain: properties of extrinsic mushroom body cells. J Comp Physiol A 154: 71-79

Smid HM, Bleeker MA, van Loon JJ, Vet, LE (2003) Three-dimensional organization of the glomeruli in the antennal lobe of the parasitoid wasps Cotesia glomerata and C. rubecula. Cell Tissue Res 312: 237-48

Simmons LW (1986) Intermale competition and mating success in the field cricket, *Gryllus bimaculatus* (De Geer). Anim Behav 34: 567-579

Skiri HT, Rø H, Berg BG, Mustaparta H (2005) Consistent organization of glomeruli in the antennal lobes of related species of Heliothin moths. J Comp Neurol 491: 367-380

Staudacher E, Gebhardt M, Dürr V (2005) Antennal movements and mechanoreception: neurobiology of active tactile sensors. Adv Insect Physiol 32: 49-205

Staudacher E, Schildberger K (1999) A newly described neuropil in the deutocerebrum of the cricket: antennal afferents and descending interneurons. Zoology 102: 212-226

Stocker RF, Lienhard MC, Borst A, Fischbach K-F (1990) Neural architecture of the antennal lobe in *Drosophila melanogaster*. Cell Tiss Res 262: 9-34

Stockinger P, Kvisiani D, Rotkopf S, Tirián L, Dickson BJ (2005) Neural circuitry that

governs *Drosophila* male courtship behavior. Cell 121: 795-807

Strausfeld NJ, Li Y (1999) Organization of olfactory and multimodal afferent neurons supplying the calyx and pedunculus of the cockroach mushroom bodies. J Comp Neurol 409: 605-625

Suzuki H (1975) Antennal movements induced by odour and central projection of the antennal neurons in the honeybee. J Insect Physiol 21: 831-847

Tregenza T, Wedell N (1997) Definitive evidence for cuticular pheromones in a cricket. Anim Behav 54 979-984

Varela N, Avilla J, Gemeno C, Anton S (2011) Ordinary glomeruli in the antennal lobe of male and female tortricid moth *Grapholita molesta* (Busck) (Lepidoptera: *Tortricidae*) process sex pheromone and host-plant volatiles. J Exp Biol 214: 637-45

Vosshall, L.B., Wong, A.M. and Axel, R. (2000). An olfactory sensory map in the fly brain. Cell 102: 147-159

Zube C, Kleineidam CJ, Kirschner S, Neef J, Rössler W (2008) Organization of the

olfactory pathway and odor processing in the antennal lobe of the ant *Camponotus floridanus*. J Comp Neurol 506: 425-441

Figure Legend

Fig. 1. Projections of the antennal sensory afferents visualized by anterograde dye filling from the antennal nerve. A: 3-D reconstruction of a cricket brain. B-E: Consecutive microscopic images from the most ventral (B) to the most dorsal part (C) of the deutocerebrum. T1 ran medially in the most ventral part of the antennal lobe (AL). The arrowhead in B indicates the terminals of one subtract of T4 in the ventral region of the protocerebrum, termed an *isthmus* (IS). T2 ran anterior boundary and T3 ran posterior boundary of the AL. Broad parallel fibers of T7 ran postero-medially into the ventral area of the flagellar afferents (VFA). T4 ran in the most dorsal part of the AL. Arrowheads in D indicate two neuropil regions in the dorsal area of the AL, termed isthmus (IS). The arrow in D indicates another subtract of T4 that terminates in the medial area of the VFA. T5 terminates in the dorsal lobe (DL, encompassed by broken line in E), where T6-1 and T6-2 were subdivided. T6-1 descended through neck connective up to the suboesophageal ganglion (SoG). T6-2 turned posteriorly and terminated in a region dorsal to the AL. F:

Terminals of T6-1 in anterior part of the ipsilateral SoG. D-F is obtained by superimposing multiple consecutive pictures. Scale bars = 100 μm. Ant: anterior, Lat: lateral.

Fig 2. Anterograde dye filling of the antennal nerve. A: Stacked images of the AL obtained from optical sections made with a CLSM. Parts of surrounded by broken line indicate glomeruli where antennal sensory afferents terminate. Fine glomerular substructures are observed in each glomerulus that is called micro-glomerular. Scale bar = 40 μm. B: A ventral view of the antennal lobe. The arrangement of T1-T4 is shown in the Suppl. 1. Scale bar = 100 μm. C: Summery of the projection of antennal sensory afferents. Broken line indicates the boundary between deutocerebrum and protocerebrum (Pr).

Fig. 3. Consecutive microscopic images of the glomeruli in the AL visualized by autofluorescence (left), and their labeled illustrations of the glomeruli (right), arranged in descending order from the ventral (A) to dorsal part (N). The interval of every consecutive

two planes is 10.4 μm. A1-D8 in right column indicates the defined name of each identified glomerulus, and the coloration reflects the group they belong to (A1-8: light blue, B1-15: yellow, C1-17: blue, D1-8: red). Scale bar = 50 μm. Ant: anterior, Lat: lateral.

Fig. 4. Ventral (A, C) and dorsal (B, D) views of the antennal lobe of male (A, B) and female cricket (C, D). Forty-nine non-sexually dimorphic glomeruli were anatomically identified in the AL. The coloration of the glomeruli reflects the group belonging to, which corresponds to that in Fig. 3. Ant: anterior, Lat: lateral.

Fig 5. A: A microscopic image of the cricket VFA, in which layers visualized by dye filling from the antennal nerve. I-V indicates layers in the VFA. Broken lines encompass the sub-compartments in the VFA. Scale bar = 50 μm. B: 3-D reconstruction of the VFA constructed by stained antennal sensory afferents. C: Measurement of fluorescent intensity. Summation of measured intensity in each 10 pixel from the base point is graphed out. I-V

indicates the peaks of fluorescent intensity, which corresponds to I-V in A. Ant: anterior, Lat: lateral.

Fig. 6. Summarized illustration of the projection patterns of the antennal sensory tracts (T1-T7) in a sagittal view of the deutocerebrum. The glomeruli in the AL were classified into 4 groups of glomeruli (A-D) by the terminals of antennal sensory tracts (T1-T4). Ventral three groups of glomeruli (A-C) were clearly separated from the dorsal group (D) (indicated by dashed line). Subtracts of T4 projected also into the protocerebrum or a part of the VFA. T5, T6-1, and T6-2 were subdivided at the entrance of the dorsal lobe (DL). T7 terminated in the VFA, forming parallel layers. Ant: anterior, Dors: dorsal.

Fig. 7. Projection neurons stained by the extracellular tracer application method in the AL. A-C: Consecutive microscopic stacked sections (ventral to dorsal) showing antenno-cerebral tracts (ACTs) originating from the AL. Four ACTs (IACT, ACT3, ACT4,

OACT) and six accessory ACTs (AACTs) were identified. Scale bars = 100 μm. D: Terminals of the AL-PNs in the anterior calyx of the mushroom body (CA). Termination area was biased in the lip region of the CA. Scale bar = 50 μm. Ant: anterior, Lat: lateral.

Fig. 8. PNs stained by the extracellular tracer application method in the VFA. A-C: Consecutive microscopic stacked sections (ventral to dorsal) showing antenno-cerebral tracts (ACTs) originating from the VFA. Three ACTs (ACT3, 4, OACT) and five accessory ACTs (AACTs) were identified. A square of broken line in B indicates the area illustrated in D. Scale bars = 100 μm. D: Terminals of side branches from the AACT3 in the anterior calyx. Scale bar = 20 μm. E: From another sample. Terminals of side branch from the OACT in the basal region of the anterior calyx. Scale bar = 50 μm. Ant: anterior, Lat: lateral.

Fig. 9. Schematic illustration of simplified antennal chemo- (A) and mechano-sensory (B)

pathways in the cricket brain. A: Chemosensory afferents terminate into the AL that consists of multiple glomeruli. The AL-PNs project through main four routes (inner route (IACT), outer route (OACT), and two middle routes (ACT3, ACT4)), and terminate into the lip region of the anterior calyx of the mushroom body (CA) and the lateral horn (LH). B: Antennal mechanosensory afferents terminates into the VFA that consists of multiple layers, where they form layers. The VFA-PNs project through three main route (outer route (OACT), and two middle routes (ACT3, ACT4)), and terminate into the basal region of the CA and the inferior and superior lateral protocerebrum (ilPr and slPr, respectively). Note that the termination areas of the chemical and tactile pathways are segregated not only in the deutocerebrum, but also in the protocerebrum.

Suppl. 1. Arrangements of T1-T4 tracts in the AL shown in Fig. 2B. Stacked images of the AL obtained from optical sections made with a CLSM and made up as a 3D animation.

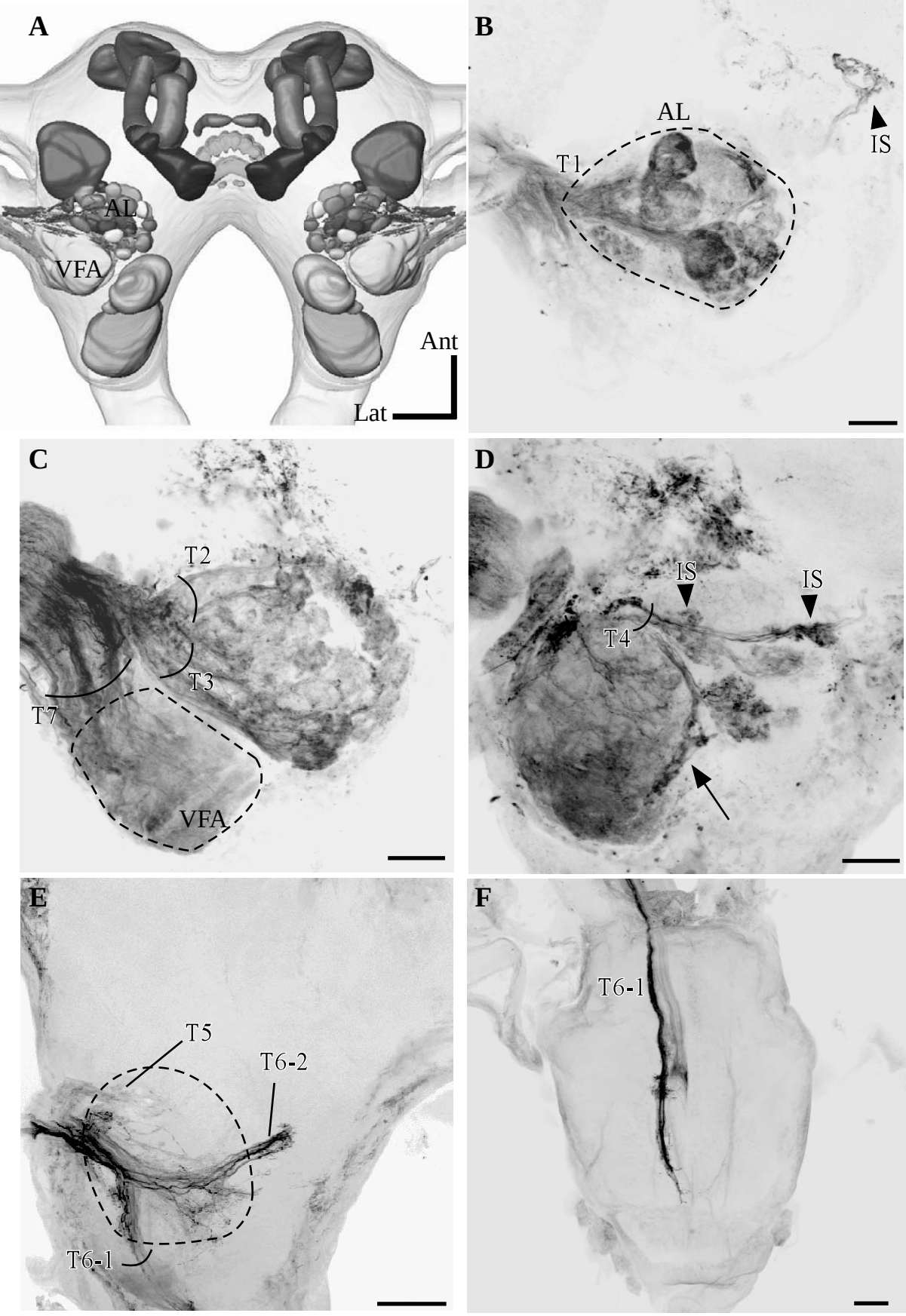

Figure 1

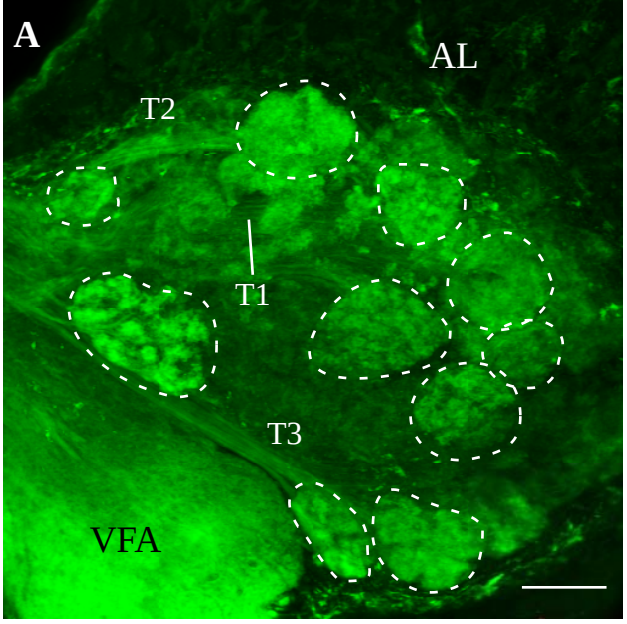
A
AL
T2
T1
T3
VFA

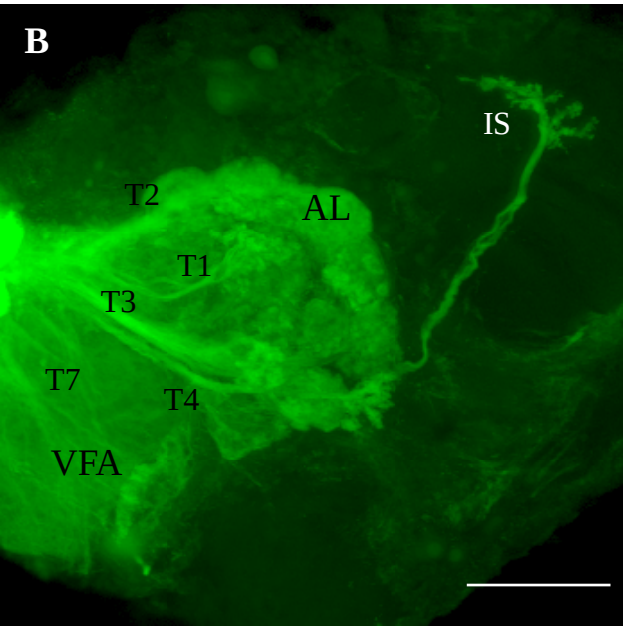
B
IS
T2
AL
T1
T3
T7
T4
VFA

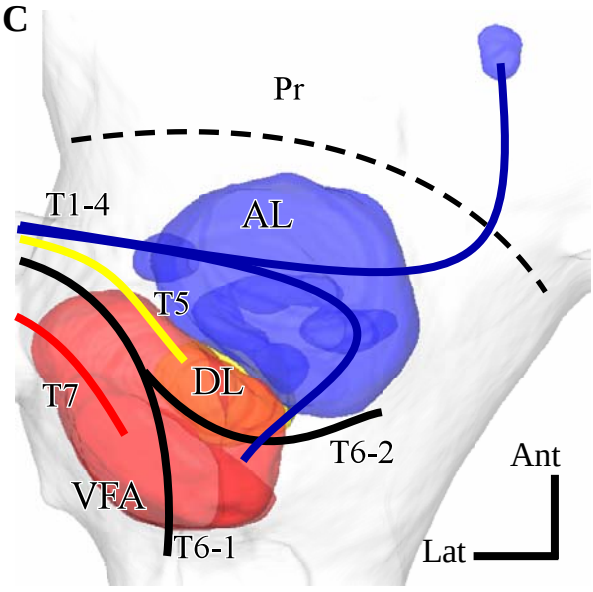
C
Pr
T1-4
AL
T5
DL
T7
T6-2
VFA
T6-1
Ant
Lat

Figure 2

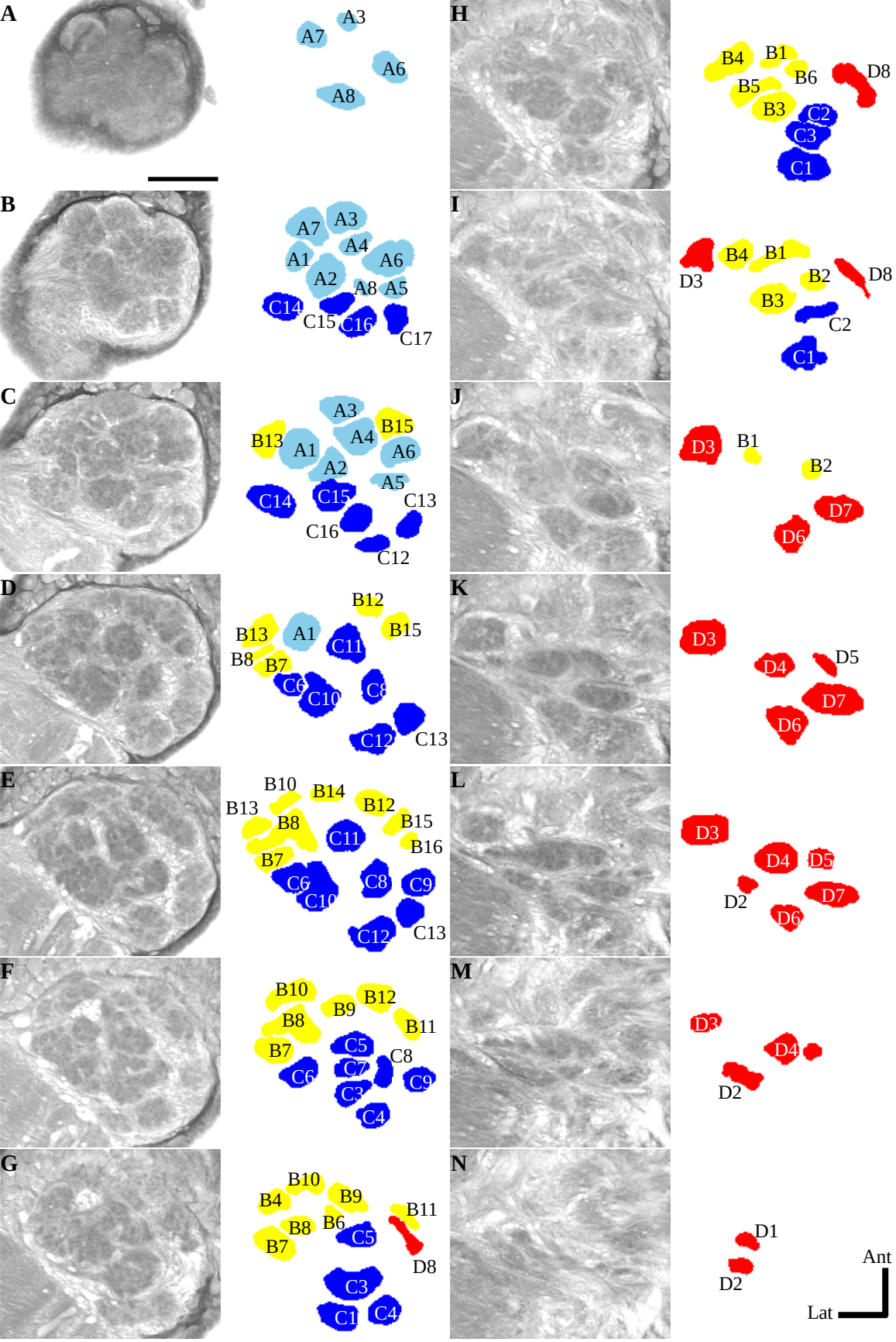
A
A3
A7
A6
A8
B
A7
A3
A4
A1
A6
A2
A8
A5
C14
C15
C16
C17
C
A3
B15
B13
A1
A4
A6
A2
A5
C14
C15
C13
C16
C12
D
B12
B15
B13
A1
C11
B8
B7
C6
C10
C8
C12
C13
E
B10
B14
B13
B12
B8
B15
C11
B16
B7
C6
C8
C9
C10
C12
C13
F
B10
B12
B8
B9
B11
B7
C5
C8
C6
C7
C9
C3
C4
G
B10
B4
B9
B11
B8
B6
C5
B7
D8
C3
C1
C4
H
B4
B1
B6
D8
B5
B3
C2
C3
C1
I
B4
B1
D3
B2
D8
B3
C2
C1
J
D3
B1
B2
D7
D6
K
D3
D4
D5
D7
D6
L
D3
D4
D5
D2
D7
D6
M
D3
D4
D2
N
D1
D2
Ant
Lat

Figure3

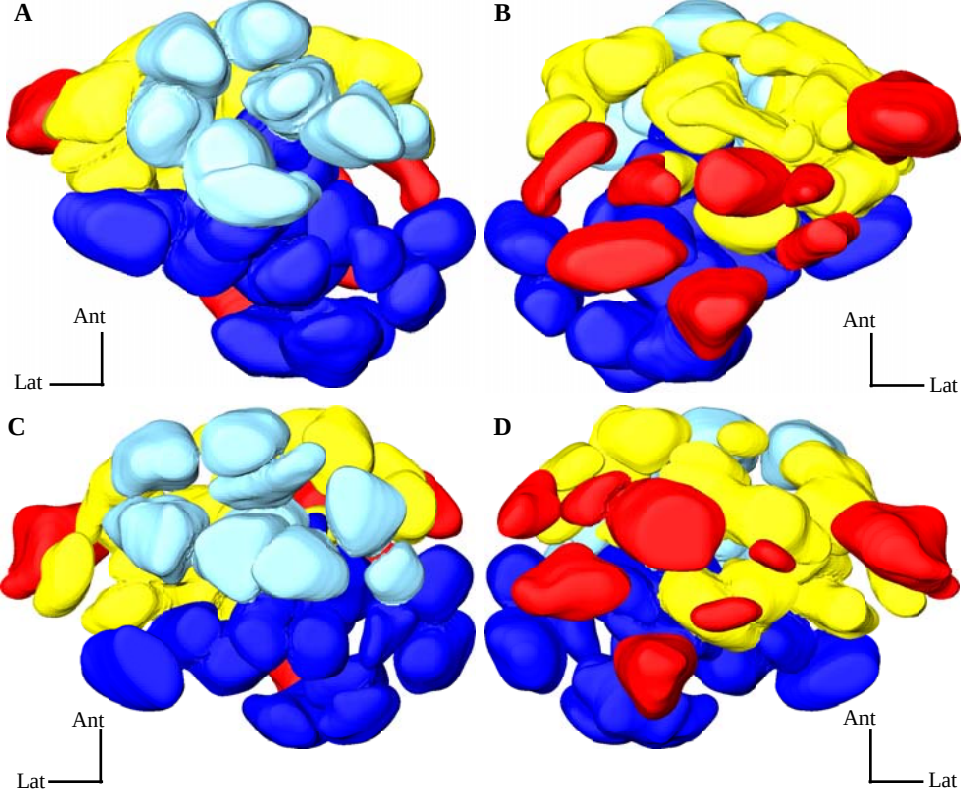

Figure4

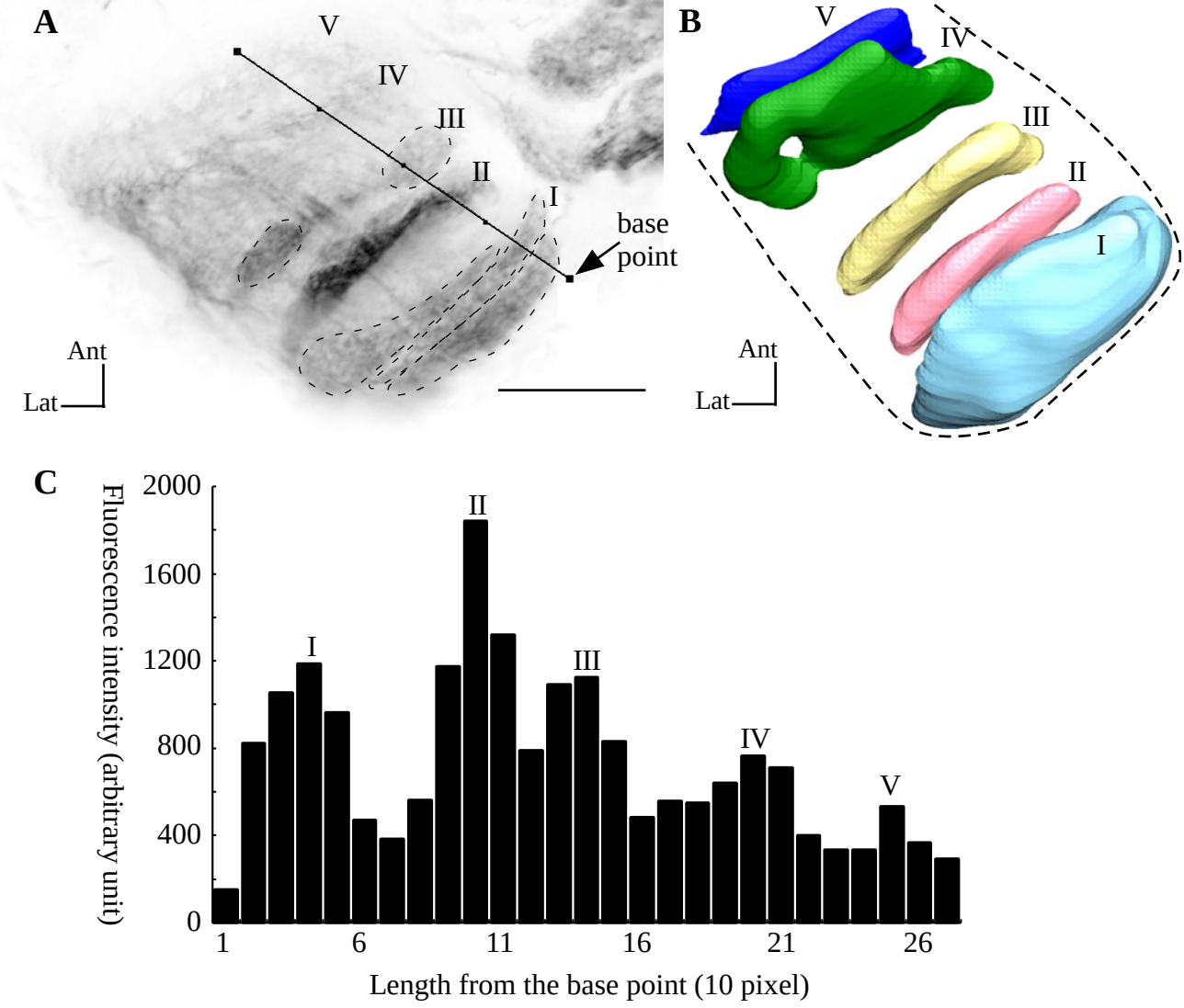
A
V
IV
III
II
I
base
point
Ant
Lat
B
V
IV
III
II
I
Ant
Lat
C
Fluorescence intensity (arbitrary unit)
2000
1600
1200
800
400
0
I
II
III
IV
V
1
6
11
16
21
26
Length from the base point (10 pixel)

Figure5

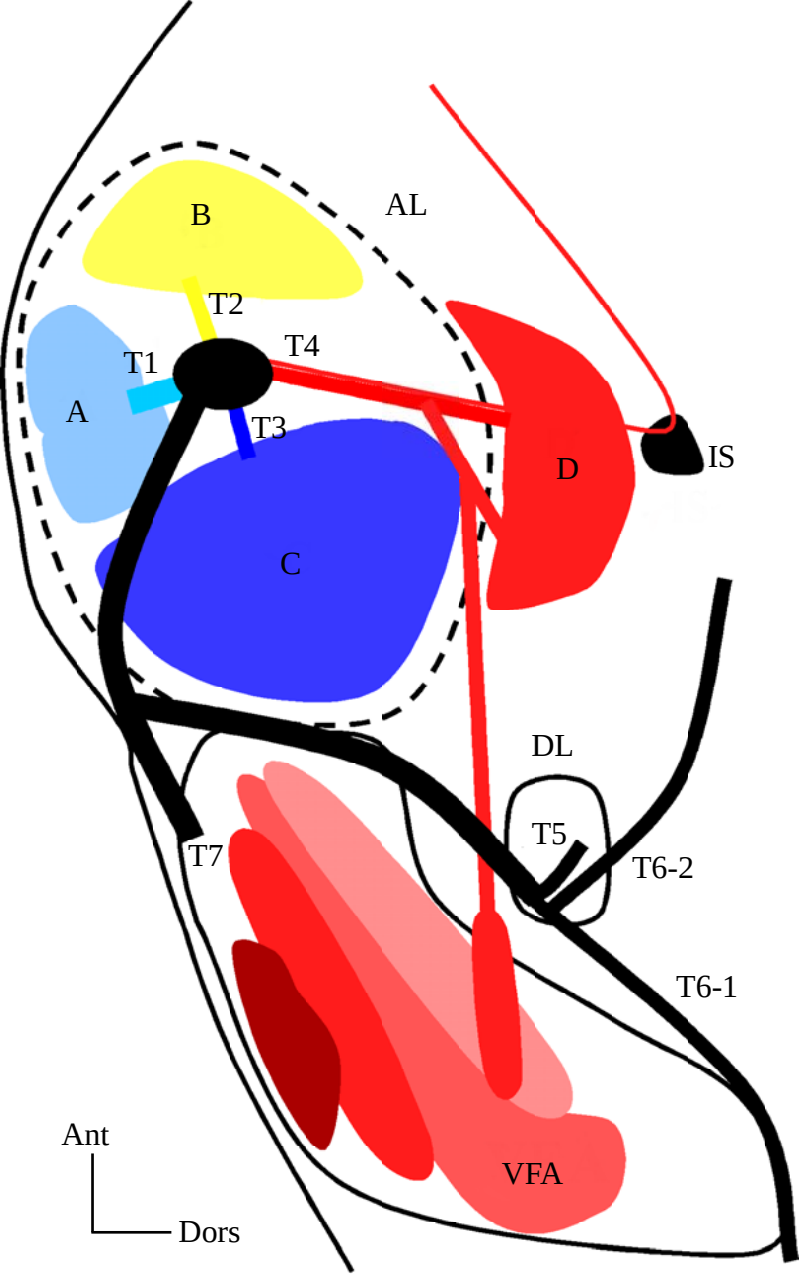

Figure6

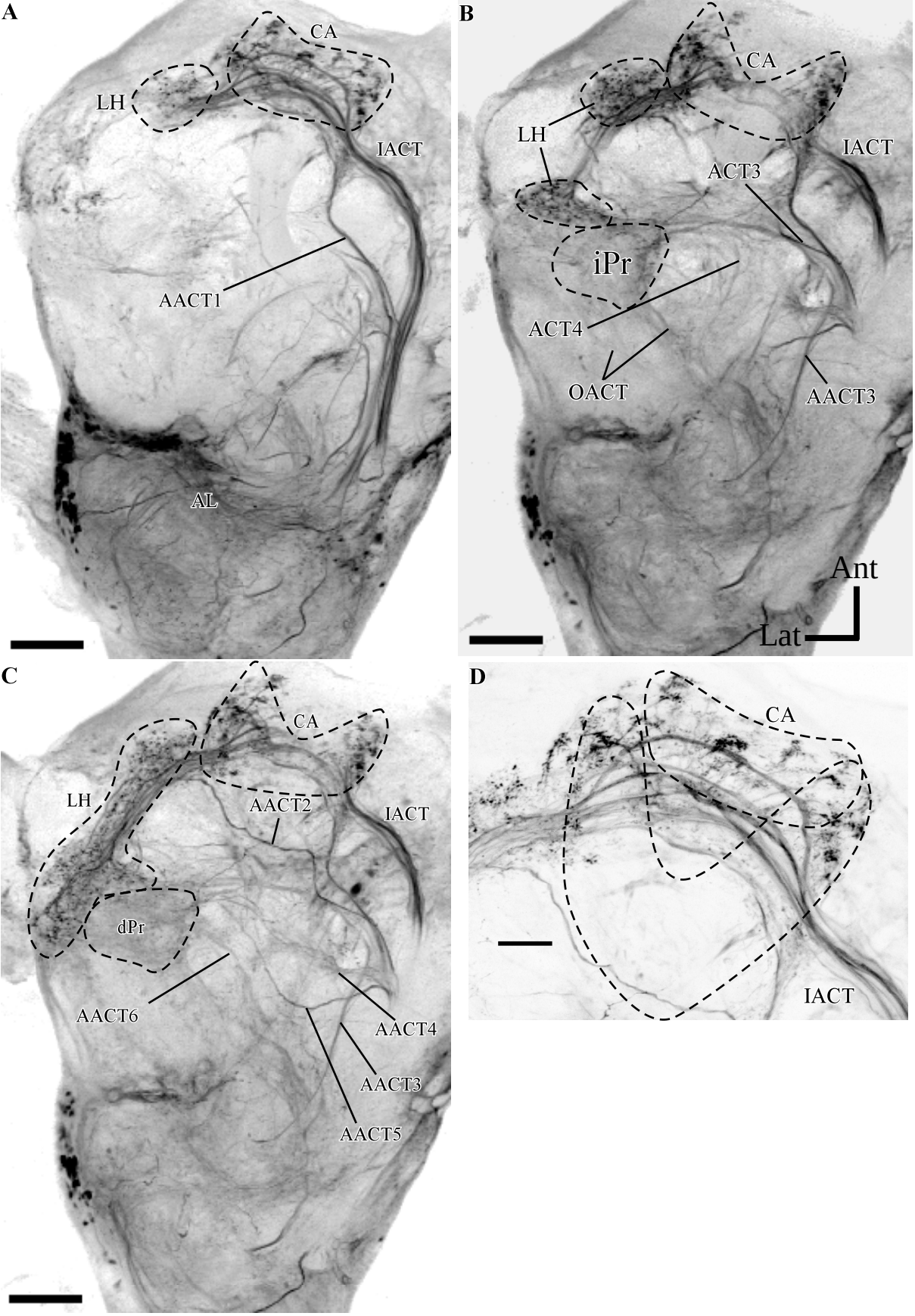
A
CA
LH
IACT
AACT1
AL
B
CA
LH
IACT
ACT3
iPr
ACT4
OACT
AACT3
Ant
Lat
C
CA
LH
AACT2
IACT
dPr
AACT6
AACT4
AACT3
AACT5
D
CA
IACT

Figure7

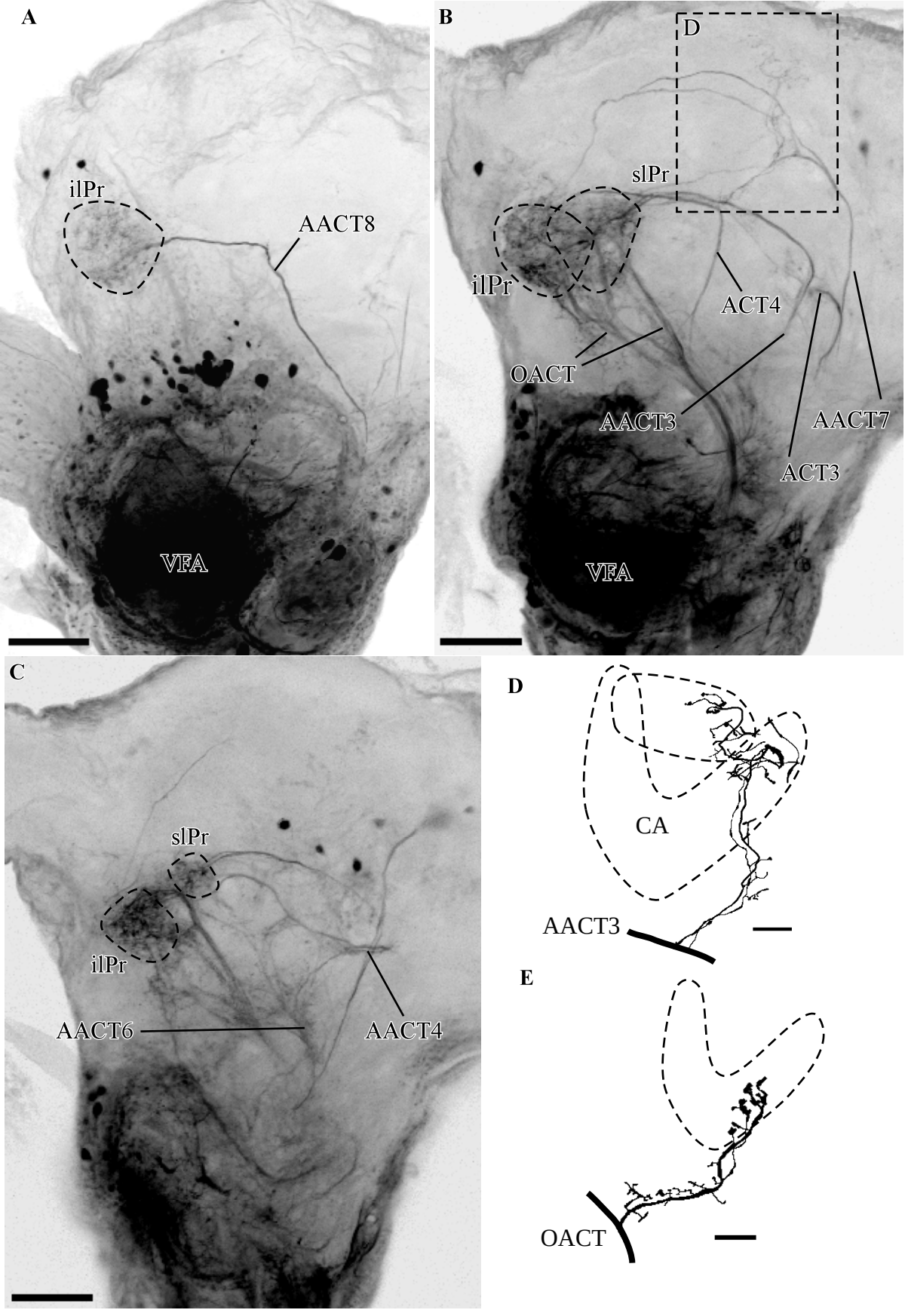
A
ilPr
AACT8
VFA
B
D
slPr
ilPr
ACT4
OACT
AACT3
AACT7
ACT3
VFA
C
slPr
ilPr
AACT6
AACT4
D
CA
AACT3
E
OACT

Figure8

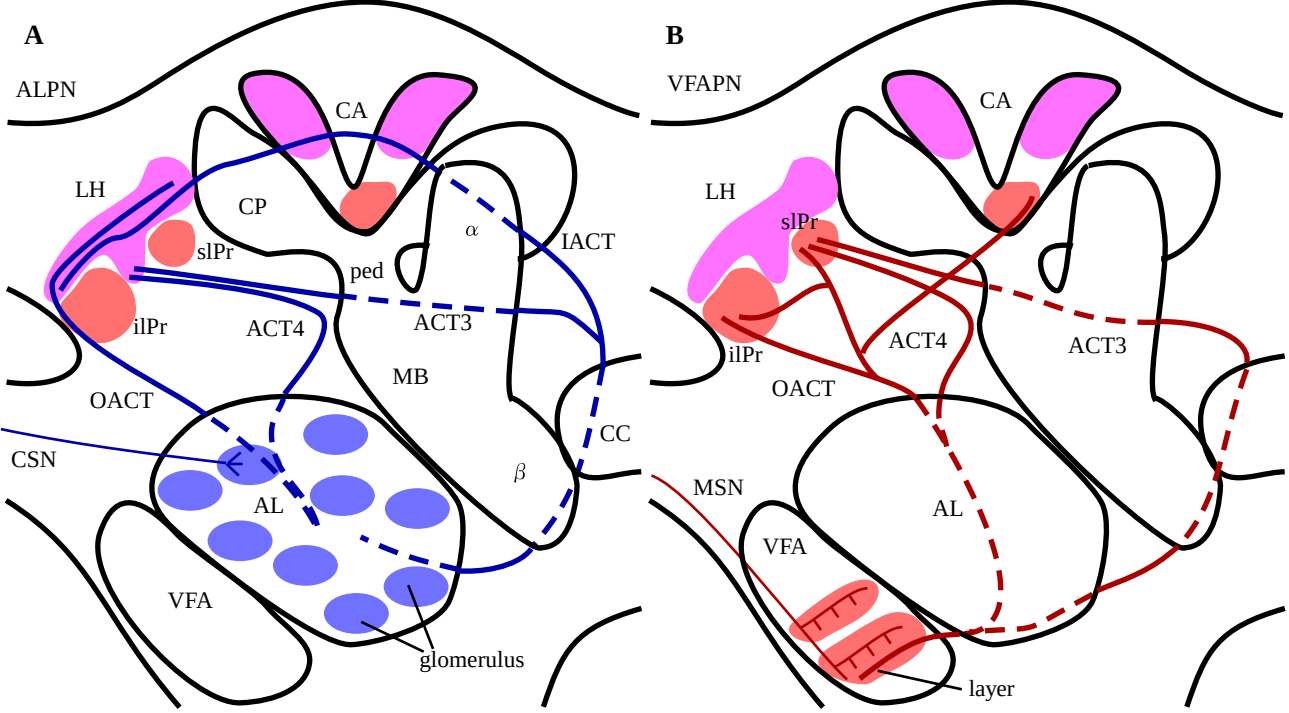
A
ALPN
CA
LH
CP
slPr
ped
α
IACT
ilPr
ACT4
ACT3
MB
OACT
CC
CSN
β
AL
VFA
glomerulus
B
VFAPN
CA
LH
slPr
ilPr
ACT4
ACT3
OACT
MSN
AL
VFA
layer

Figure9